A Theoretical Framework for Chimera Domain Decomposition

S. L. Keeling*
Sverdrup Technology, Inc./AEDC Group, Arnold Air Force Base, TN 37389

R. W. Tramel† and J. A. Benek‡
Micro Craft Inc., Tullahoma, TN 37388

Advances in Flow Simulation Techniques–a Conference Dedicated to the Memory of Professor Joseph L. Steger, UC Davis, May 2-4, 1997.

1 Introduction.

The Chimera scheme is a domain decomposition methodology developed for the solution of systems of partial differential equations [1]. In particular, the scheme has been used extensively to numerically solve the conservation laws of fluid dynamics [2], [3], [4]. The advantages of domain decomposition methods include the following. First, a very large computational problem is partitioned into a set of smaller problems in such a way that none of the smaller problems exhausts available computer memory. Also, the partitioning provides a natural coarse grain structure for parallel computing. Finally, mesh generation is easier since the field around a complex geometry is divided into simply shaped regions. Unlike other approaches [5], the Chimera method simplifies mesh generation greatly since it permits decompositions with overlapping subdomains.

A domain decomposition method is defined not only by the geometric criteria by which the global domain is partitioned, but also by the manner of information transfer among subdomains. Specifically, in place of the global boundary value problem, separate boundary value problems must be posed on each subdomain. On a given subdomain, values imposed on a new or artificial boundary are obtained from a contiguous or overlapping subdomain. In this way the separate boundary value problems are coupled. A numerical solution to the coupled system is usually obtained iteratively by applying the Schwarz Alternating Procedure [6]. The important point to emphasize is that the success of a domain decomposition method depends heavily on the way values are transferred to artificial boundaries.

For example, Benek et al., applied the Chimera approach to solving the Euler equations numerically for the transonic flow over an airfoil [2]. They obtained flow fields that differed significantly, depending upon whether a single domain or multiple overlapping subdomains were used. It was later realized that anomalies in the Chimera flow field were related to a drop in the order of dissipation near artificial boundaries. Rai speculated that the discrepancy resulted from the non-conservative nature of the interpolation scheme used to compute artificial boundary data [7]. He developed an alternate interpolation method for the fluxes at the boundaries of contiguous disjoint subdomains. Subsequently, several authors extended this approach [8], [9] or developed alternate approaches [10], [11], [12] for non-disjoint subdomains. None of these approaches has been completely successful in avoiding errors introduced by the transfer of values at artificial boundaries. Also, in the absence of a clearly articulated mathematical framework, the controversy and speculation about the nature of these errors continues.

The primary purpose of this paper is to introduce a new mathematical framework within which Chimera schemes can be properly analyzed. Previous analyses have fallen short of this goal because single domain concepts and perspectives have been imposed upon an inherently more general class of problems. In particular, distinctions are made here between the system of partial differential equations posed for a single domain and the system posed for multiple overlapping domains. As a result, the boundary operator required for the proper transfer of values at artificial boundaries is identified. Then, an appropriate numerical approximation to this operator is proposed. In this framework, it becomes clear that discrete conservation in a piecewise sense can be sufficient for Chimera approximations to converge properly with respect to mesh refinement.

The secondary purpose of this paper is to clarify the nature of the numerical errors observed with the Chimera scheme. On the one hand, a poor approximation to the boundary operator, mentioned above, corrupts the solution in a way that is necessarily linked with the domain decomposition technique. On the other hand, certain numerical phenomena have been mistakenly attributed to some non-conservative aspect of the Chimera scheme. Such phenomena are readily identified if they can be shown to be as much an issue in a single domain context as they are in the context of multiple overlapping subdomains.

2 Generalized Solutions.

The purpose of this section is to clarify what is meant by a solution to a system of partial differential equations both in a single domain context and in the context of multiple overlapping subdomains. Particular focus is placed on systems of conservations laws of interest in fluid dynamics.

*Engineering Specialist.
†Analysis Engineer.
‡Director, Integrated Testing and Evaluation Operations.

Because of the nonlinear nature of the Euler and compressible Navier-Stokes equations, smooth solutions are generally limited to small time strips near smooth initial data. For larger values of time, the solutions tend to form discontinuities. Thus, the notion of solution must be generalized to a distributional setting. These non-classical solutions are, in general, not unique. On the other hand, Lax and Wendroff have shown that, for scalar conservation laws, uniqueness can be established in a restricted class of *entropy-satisfying* distributional solutions [13]. Related results have been obtained for more complex but incomplete models of fluid flow [14], [15], [16]. However, there is evidence that even entropy-satisfying solutions of the Euler equations are not unique [17]. Unfortunately, the proper setting to establish well-posedness for systems such as the Euler equations or the compressible Navier-Stokes equations remains elusive. Therefore, new definitions are given below to accommodate the most general cases.

2.1 Single Domain.

Systems of conservation laws of interest in fluid dynamics can be written in a classical differential form as,

$$(1) \qquad \begin{cases} \partial_t \boldsymbol{Q} &= -\nabla \cdot \boldsymbol{F}(\boldsymbol{Q}), & \Omega \times [0,T] \\ \boldsymbol{Q} &= \boldsymbol{Q}_B, & \partial\Omega \times [0,T] \\ \boldsymbol{Q} &= \boldsymbol{Q}_0, & \Omega \times \{0\}. \end{cases}$$

Here, Ω is a bounded domain in $\boldsymbol{R}^N$ with a well-behaved boundary, $\partial\Omega$, and $\nabla = (\partial_{x_1}, \ldots, \partial_{x_N})$. The vector of conserved quantities is denoted by $\boldsymbol{Q}$. Also, $\boldsymbol{F}$ is a collection of flux vectors, $(\boldsymbol{F}_1, \ldots, \boldsymbol{F}_N)$, which are assumed to be smooth, nonlinear functions of $\boldsymbol{Q}$. The initial values of $\boldsymbol{Q}$ are denoted by $\boldsymbol{Q}_0$ and the boundary values on $\partial\Omega$ by $\boldsymbol{Q}_B$. The boundary values, $\boldsymbol{Q}_B$, are only relevant when the local characteristics allow information on the boundary to propagate into the interior of the domain.

Because the solutions of interest possess discontinuities, an integral form of the conservation laws will be considered in place of the differential form. The integral form is derived by integrating Eq. (1) over a cylindrical space-time region, $C = D \times [t_1, t_2]$, and applying the divergence theorem to obtain,

$$(2) \qquad \int_D [\boldsymbol{Q}(t_2) - \boldsymbol{Q}(t_1)] + \int_{\partial D \times [t_1,t_2]} \boldsymbol{F}(\boldsymbol{Q}) \cdot \hat{\boldsymbol{n}} = 0.$$

Here, D is any domain in Ω with well-behaved boundary, ∂D, and $\hat{\boldsymbol{n}}$ is a unit normal vector which is outwardly directed with respect to D. Also, $[t_1, t_2]$ is any interval in $[0, T]$. Even though differentiability is not imposed on $\boldsymbol{Q}$ in this equation, more subtle properties are implicitly imposed on $\boldsymbol{Q}$ by the integral form. For example, since $\boldsymbol{Q}$ can be discontinuous across the boundary of the space-time region, C, its boundary values are ambiguous in the above integration. A natural approach to resolving this ambiguity is to understand $\boldsymbol{Q}$ over ∂C as a kind of one-sided limit from inside C. This limit can be made rigorous to give what is known as the *trace* of $\boldsymbol{Q}$ on ∂C with respect to C. (For details, see, e.g., Ref. [18].) The existence of trace values requires that $\boldsymbol{Q}$ be sufficiently well-behaved near ∂C. A natural class of functions having these properties is the space of functions with bounded variation in $\Omega \times [0, T]$. The notion of trace values will become especially important in the discussion of multiple overlapping subdomains.

A generalization of the classical solution can now be defined as follows. A function $\boldsymbol{Q}$ with bounded variation in $\Omega \times [0, T]$ is said to be a *weak solution* to Eq. (1) if for every domain $D \subset \Omega$ with a well-behaved boundary, ∂D, and for every $[t_1, t_2] \subset [0, T]$,

$$(3) \qquad \int_D [\mathcal{T}\boldsymbol{Q}(t_2) - \mathcal{T}\boldsymbol{Q}(t_1)] + \int_{\partial D \times [t_1,t_2]} \boldsymbol{F}(\mathcal{T}\boldsymbol{Q}) \cdot \hat{\boldsymbol{n}} = 0$$

where $\mathcal{T}\boldsymbol{Q}$ denotes the trace of $\boldsymbol{Q}$ with respect to $D \times [t_1, t_2]$. As a consequence of the smoothness of $\boldsymbol{F}$, $\boldsymbol{F}(\mathcal{T}\boldsymbol{Q}) = \mathcal{T}\boldsymbol{F}(\boldsymbol{Q})$. If the boundary of $D \times [t_1, t_2]$ partially coincides with the boundary of the global domain, then in accordance with Eq. (1), the following are used in place of $\mathcal{T}\boldsymbol{Q}$ in Eq. (3),

$$(4) \qquad \mathcal{T}\boldsymbol{Q} = \begin{cases} \boldsymbol{Q}_B, & \partial\Omega \times [0,T] \\ \boldsymbol{Q}_0, & \Omega \times \{0\}. \end{cases}$$

It can be shown that a distributional solution with bounded variation is a weak solution in the above sense and vice versa [19], [20].

2.2 Multiple Overlapping Domains.

Now let the system of conservation laws be posed as follows in a differential form on multiple overlapping subdomains, $\{\Omega^{(i)}\}_{i=1}^I$, such that $\Omega = \cup_{i=1}^I \Omega^{(i)}$,

$$(5) \qquad \begin{cases} \partial_t \boldsymbol{Q}^{(i)} &= -\nabla \cdot \boldsymbol{F}(\boldsymbol{Q}^{(i)}), & \Omega^{(i)} \times [0,T] \\ \boldsymbol{Q}^{(i)} &= \boldsymbol{Q}^{(j)}, & \gamma_i^j \times [0,T] \\ \boldsymbol{Q}^{(i)} &= \boldsymbol{Q}_B, & [\partial\Omega^{(i)} \cap \partial\Omega] \times [0,T] \\ \boldsymbol{Q}^{(i)} &= \boldsymbol{Q}_0, & \Omega^{(i)} \times \{0\} \\ & & i = 1, \ldots, I. \end{cases}$$

Here, γ_i^j is the subset of $\partial\Omega^{(i)} \cap \Omega^{(j)}$ where boundary values are supplied from $\Omega^{(j)}$. For a given point in $\partial\Omega^{(i)}$, there may be many choices for the index, j. Thus, γ_i^j need not coincide with $\partial\Omega^{(i)} \cap \Omega^{(j)}$. It should be emphasized that the coupling among subdomains through the selection of the sets, $\{\gamma_i^j\}$, is an ingredient of the problem statement in Eq. (5). Again, the values imposed on these artificial boundaries are only relevant when the characteristics allow information to propagate into the interior of the subdomain. The authors are unaware of any general studies of the existence of solutions to Eq. (5).

A generalized notion of solution which admits discontinuities will now be developed for the above coupled system of equations. For fixed i and given $\boldsymbol{Q}^{(j)}$, a function $\boldsymbol{Q}^{(i)}$ with bounded variation in $\Omega^{(i)} \times [0, T]$ is a weak solution to the ith portion of the system in Eq. (5) if for every regular domain $D \subset \Omega^{(i)}$ and every interval $[t_1, t_2] \subset [0, T]$,

$$(6) \qquad \int_D [\mathcal{T}\boldsymbol{Q}^{(i)}(t_2) - \mathcal{T}\boldsymbol{Q}^{(i)}(t_1)] + \int_{\partial D \times [t_1,t_2]} \boldsymbol{F}(\mathcal{T}\boldsymbol{Q}^{(i)}) \cdot \hat{\boldsymbol{n}} = 0$$

where $\mathcal{T}\boldsymbol{Q}^{(i)}$ denotes the trace of $\boldsymbol{Q}^{(i)}$ with respect to $D \times [t_1, t_2]$. If the boundary of $D \times [t_1, t_2]$ partially coincides with artificial or global domain boundaries, then in accordance with Eq. (5), the following are used in place of $\mathcal{T}\boldsymbol{Q}^{(i)}$ in Eq. (6),

$$(7) \qquad \mathcal{T}\boldsymbol{Q}^{(i)} = \begin{cases} \mathcal{T}\boldsymbol{Q}^{(j)}, & \gamma_i^j \times [0,T] \\ \boldsymbol{Q}_B, & [\partial\Omega^{(i)} \cap \partial\Omega] \times [0,T] \\ \boldsymbol{Q}_0, & \Omega^{(i)} \times \{0\}. \end{cases}$$

Because weak solutions of Eq. (1) may not be unique, $\boldsymbol{Q}^{(i)}$ cannot be expected to be equal to $\boldsymbol{Q}^{(j)}$ in regions where $\Omega^{(i)}$ and $\Omega^{(j)}$ overlap. Thus, the collection of functions, $\{\boldsymbol{Q}^{(i)}\}_{i=1}^{I}$, will be called a *multi-valued weak solution* to the complete coupled system in Eq. (5).

As a result of the substitution in Eq. (7), the generalized boundary condition for $\boldsymbol{Q}^{(i)}$ in terms of $\boldsymbol{Q}^{(j)}$ is that,

$$\mathcal{T}_i\boldsymbol{Q}^{(i)} \quad = \quad \mathcal{T}_i\boldsymbol{Q}^{(j)}, \quad \gamma_i^j \times [0,T] \tag{8}$$

where $\mathcal{T}_i$ denotes the trace operator with respect to $\Omega^{(i)} \times [0,T]$. It is important to emphasize that the trace operator is directional and, in general, the trace values of $\boldsymbol{Q}^{(j)}$ from opposite sides of γ_i^j are not equal. The boundary condition for $\boldsymbol{Q}^{(i)}$ is written in terms of trace values of $\boldsymbol{Q}^{(j)}$ from only one side of γ_i^j and not some average of trace values from both sides. The important consequences of this formulation will be seen below.

A weak solution, $\boldsymbol{Q}$, to Eq. (1) also solves Eq. (5) in a weak sense with $\boldsymbol{Q}^{(i)} = \boldsymbol{Q}$, $i = 1, \ldots, I$. On the other hand, care must be taken to construct a single-valued weak solution to Eq. (1) from a multi-valued weak solution to Eq. (5). This point is illustrated in the following example.

Let $I = 3$ so that $\Omega = \Omega^{(1)} \cup \Omega^{(2)} \cup \Omega^{(3)}$ as shown in Fig. 1. As explained earlier, there are many ways to establish the

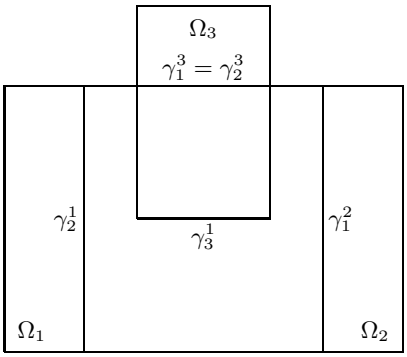

Figure 1: Overlapping subdomains.

connectivity among subdomains through the specification of the artificial boundaries, $\{\gamma_i^j\}$. Here, suppose the $\boldsymbol{Q}^{(1)}$ boundary values are given by $\mathcal{T}_1\boldsymbol{Q}^{(2)}$ and $\mathcal{T}_1\boldsymbol{Q}^{(3)}$ along γ_1^2 and γ_1^3, respectively. Also, let the $\boldsymbol{Q}^{(2)}$ boundary values be specified by $\mathcal{T}_2\boldsymbol{Q}^{(1)}$ and $\mathcal{T}_2\boldsymbol{Q}^{(3)}$ along γ_2^1 and γ_2^3, respectively. Finally, assume the $\boldsymbol{Q}^{(3)}$ boundary values are given by $\mathcal{T}_3\boldsymbol{Q}^{(1)}$ along γ_3^1. Then, as illustrated in Fig. 2, a global solution, $\boldsymbol{Q}$, can be constructed as follows,

$$\boldsymbol{Q} \quad = \quad \begin{cases} \boldsymbol{Q}^{(1)}, & \Omega^{(1)} \\ \boldsymbol{Q}^{(2)}, & \Omega^{(2)} - \Omega^{(1)} \\ \boldsymbol{Q}^{(3)}, & \Omega^{(3)} - \Omega^{(2)} - \Omega^{(1)}. \end{cases} \tag{9}$$

This $\boldsymbol{Q}$ is found to be a weak solution to Eq. (1) as follows. Let D be an arbitrary regular domain in Ω and $[t_1, t_2]$ an arbitrary interval in $[0,T]$. Clearly, if D does not overlap $\partial\Omega^{(i)}$ for any i, then Eq. (3) follows from Eqs. (6) and (9). On the other hand, suppose that D overlaps a boundary as shown in Fig. 2. Then Eq. (3) is established by dividing D into a left portion, $D_l = D \cap \Omega^{(1)}$, and a right portion, $D_r = D \cap \Omega^{(2)}$. Take $\hat{\boldsymbol{n}}_l$

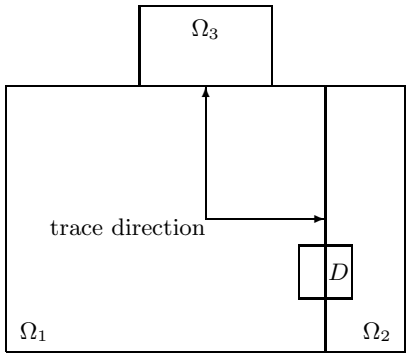

Figure 2: Single-valued solution.

and $\hat{\boldsymbol{n}}_r$ to represent unit normal vectors which are outwardly directed with respect to D_l and D_r, respectively. Let the subset of γ_1^2 separating D_l and D_r be designated as γ. Also, let the trace operators for $D_l \times [t_1, t_2]$ and $D_r \times [t_1, t_2]$ be denoted by $\mathcal{T}_l$ and $\mathcal{T}_r$, respectively. Then

$$\begin{aligned}
&\int_D [\mathcal{T}\boldsymbol{Q}(t_2) - \mathcal{T}\boldsymbol{Q}(t_1)] + \int_{\partial D \times [t_1,t_2]} \boldsymbol{F}(\mathcal{T}\boldsymbol{Q}) \cdot \hat{\boldsymbol{n}} \\
&= \int_{D_l} [\mathcal{T}_l\boldsymbol{Q}^{(1)}(t_2) - \mathcal{T}_l\boldsymbol{Q}^{(1)}(t_1)] + \int_{\partial D_l \times [t_1,t_2]} \boldsymbol{F}(\mathcal{T}_l\boldsymbol{Q}^{(1)}) \cdot \hat{\boldsymbol{n}}_l \\
&+ \int_{D_r} [\mathcal{T}_r\boldsymbol{Q}^{(2)}(t_2) - \mathcal{T}_r\boldsymbol{Q}^{(2)}(t_1)] + \int_{\partial D_r \times [t_1,t_2]} \boldsymbol{F}(\mathcal{T}_r\boldsymbol{Q}^{(2)}) \cdot \hat{\boldsymbol{n}}_r \\
&- \int_{\gamma \times [t_1,t_2]} \boldsymbol{F}(\mathcal{T}_l\boldsymbol{Q}^{(1)}) \cdot \hat{\boldsymbol{n}}_l - \int_{\gamma \times [t_1,t_2]} \boldsymbol{F}(\mathcal{T}_r\boldsymbol{Q}^{(2)}) \cdot \hat{\boldsymbol{n}}_r \\
&= - \int_{\gamma \times [t_1,t_2]} \boldsymbol{F}(\mathcal{T}_l\boldsymbol{Q}^{(2)}) \cdot \hat{\boldsymbol{n}}_l - \int_{\gamma \times [t_1,t_2]} \boldsymbol{F}(\mathcal{T}_r\boldsymbol{Q}^{(2)}) \cdot \hat{\boldsymbol{n}}_r.
\end{aligned}$$

Observe that integrations along γ are added in the second and third lines and later subtracted in the fourth. Then, Eq. (6) is used to eliminate terms on the second and third lines. Also, note the use of the fact that $\mathcal{T}_l\boldsymbol{Q}^{(1)} = \mathcal{T}_l\boldsymbol{Q}^{(2)}$ on γ. This follows since, according to Eq. (8), $\mathcal{T}_1\boldsymbol{Q}^{(1)} = \mathcal{T}_1\boldsymbol{Q}^{(2)}$ on γ_1^2. (The importance of this boundary condition formulation can now be seen as advertised following Eq. (8).) Finally, the right side above is seen to be zero as follows. If the above calculation is performed starting with $\boldsymbol{Q}^{(2)}$ instead of $\boldsymbol{Q}$, the first line is zero according to Eq. (6). Also, the same bottom line is reached with the repeated use of Eq. (6). Thus, Eq. (3) is obtained. A similar calculation can be performed with respect to γ_1^3. Therefore, $\boldsymbol{Q}$ is a weak solution to Eq. (1).

Note that it is possible to construct other single-valued functions from $\boldsymbol{Q}^{(1)}$, $\boldsymbol{Q}^{(2)}$, and $\boldsymbol{Q}^{(3)}$, which are not global weak solutions. Furthermore, it is possible to specify the sets $\{\gamma_i^j\}$ so that no manipulations of a multi-valued weak solution can be performed to create a global weak solution. Nevertheless, a specification of connectivities, $\{\gamma_i^j\}$, can always be found which permits the construction of a global solution. Specifically, this fact is demonstrated by following the pattern of the above ex-

ample. Suppose the sets, $\{\gamma_i^j\}$, are prescribed to satisfy,

$$\partial\left[\bigcup_{k=1}^{j-1}\Omega^{(k)}\right]\cap\partial\Omega^{(i)}\cap\Omega^{(j)}\subset\gamma_i^j,\quad 1\le i<j\le I.$$

Then the following is a global solution,

$$\boldsymbol{Q}=\boldsymbol{Q}^{(i)}\text{ in }\Omega^{(i)}-\bigcup_{j=1}^{i-1}\Omega^{(j)},\quad i=1,\ldots,I.$$

3 Numerical Approximations.

The purpose of this section is to formulate general discretizations of the systems of the previous section and to clarify numerical issues surrounding the discrete formulations. Particular focus is placed on discrete conservation in a two-fold manner. First, it is recognized that the trace operator is the boundary operator to approximate for the proper transfer of values at artificial boundaries. An appropriate numerical approximation to this operator is proposed as an alternative to error-prone data transfer schemes used previously. Second, it is explained that certain numerical phenomena have been mistakenly attributed to some non-conservative aspect of the Chimera scheme. Such phenomena are readily identified if they can be shown to be as much an issue in a single domain context as they are in the context of multiple overlapping subdomains.

3.1 Single Domain.

Using the finite volume technique, the following discrete form of Eq. (1) is obtained,

$$\text{(10)}\quad\begin{cases} V_{\mathbf{j}}[\boldsymbol{q}_{\mathbf{j}}^{n+1}-\boldsymbol{q}_{\mathbf{j}}^{n}] &= -\Delta t\displaystyle\sum_{|\mathbf{k}|=1}\boldsymbol{f}_{\mathbf{j}+\frac{1}{2}\mathbf{k}}^{n+\frac{1}{2}}\cdot\hat{\boldsymbol{n}}_{\mathbf{j}+\frac{1}{2}\mathbf{k}},\\ & \qquad D_{\mathbf{j}}\in\Omega,\quad t^{n+1}\in[0,T]\\ \boldsymbol{f}_{\mathbf{j}+\frac{1}{2}\mathbf{k}}^{n+\frac{1}{2}} &= \boldsymbol{F}(\boldsymbol{Q}_B(\boldsymbol{x}_{\mathbf{j}+\frac{1}{2}\mathbf{k}},t^{n+\frac{1}{2}})),\\ & \qquad \boldsymbol{x}_{\mathbf{j}+\frac{1}{2}\mathbf{k}}\in\partial\Omega,\quad t^{n+\frac{1}{2}}\in[0,T]\\ \boldsymbol{q}_{\mathbf{j}}^{0} &= \boldsymbol{Q}_0(\boldsymbol{x}_{\mathbf{j}},0),\\ & \qquad \boldsymbol{x}_{\mathbf{j}}\in\Omega,\quad t=0. \end{cases}$$

Here, $\mathbf{j}$ and $\mathbf{k}$ are multi-indices. Specifically, $\mathbf{j}=(j_1,\ldots,j_N)$ and $\mathbf{k}=(k_1,\ldots,k_N)$ for integers $\{j_i\}_{i=1}^N$ and $\{k_i\}_{i=1}^N$. Also, $|\mathbf{k}|$ is defined as $\sum_{i=1}^N|k_i|$. Thus, the condition, $|\mathbf{k}|=1$, constrains the components of $\mathbf{k}$ to be ±1. For example, $\mathbf{k}=(-1,0,\ldots,0)$ satisfies $|\mathbf{k}|=1$ and $\mathbf{j}+\frac{1}{2}\mathbf{k}=(j_1-\frac{1}{2},j_2,\ldots,j_N)$. The cell, $D_{\mathbf{j}}$ has volume, $V_{\mathbf{j}}$, and faces with outward pointing normal vectors, $\hat{\boldsymbol{n}}_{\mathbf{j}+\frac{1}{2}\mathbf{k}}$, $|\mathbf{k}|=1$. These normal vectors have magnitudes equal to the areas of the respective faces. The center of the cell, $D_{\mathbf{j}}$, is located at $\boldsymbol{x}_{\mathbf{j}}$ and the centers of the cell faces at $\boldsymbol{x}_{\mathbf{j}+\frac{1}{2}\mathbf{k}}$, $|\mathbf{k}|=1$. Finally, t^n is the time at the nth time level, $t^{n+\frac{1}{2}}=\frac{1}{2}(t^n+t^{n+1})$, and $\Delta t=t^{n+1}-t^n$.

The dependent variables, $\boldsymbol{q}_{\mathbf{j}}^n$, approximate the average of $\boldsymbol{Q}$ over $D_{\mathbf{j}}$ at time t^n. The numerical flux, $\boldsymbol{f}_{\mathbf{j}+\frac{1}{2}\mathbf{k}}^{n+\frac{1}{2}}$, approximates the average of $\boldsymbol{F}(\boldsymbol{Q})$ over the time interval $[t^n,t^{n+1}]$ and over the face of $D_{\mathbf{j}}$ at $\boldsymbol{x}_{\mathbf{j}+\frac{1}{2}\mathbf{k}}$. For this approximation, $\boldsymbol{f}_{\mathbf{j}+\frac{1}{2}\mathbf{k}}^{n+\frac{1}{2}}$ may depend upon several values of $\boldsymbol{q}$ in a neighborhood of $\boldsymbol{x}_{\mathbf{j}+\frac{1}{2}\mathbf{k}}$. Thus, the condition involving $\boldsymbol{Q}_B$ in Eq. (10) may involve interior $\boldsymbol{q}$ values in addition to $\boldsymbol{Q}_B$ values on the boundary. Specific numerical models are distinguished by the choice of numerical flux function. Also, Eq. (10) does not represent the most general method of temporal differencing.

For systems of conservation laws, there are presently no general theorems that guarantee the convergence of discretizations with respect to space-time mesh refinement. Existing convergence theorems for scalar conservation laws require conditions such as consistency, stability, total variation stability, monotonicity, etc. (See, e.g., Refs. [16], [19], and [20].) In addition, entropy conditions are imposed to achieve convergence to a physically appropriate solution. A condition often rigidly imposed in these theorems is that the numerical scheme have none other than the structure shown in Eq. (10) so that a kind of discrete conservation results. Specifically, if the terms in Eq. (10) are summed over cells, $D_{\mathbf{j}}$, in a region, $D\subset\Omega$, fluxes for opposite sides of interior cells cancel in a telescoping fashion and only the fluxes on ∂D remain,

$$\text{(11)}\quad\sum_{D_{\mathbf{j}}\in D}V_{\mathbf{j}}\boldsymbol{q}_{\mathbf{j}}^{n+1}=\sum_{D_{\mathbf{j}}\in D}V_{\mathbf{j}}\boldsymbol{q}_{\mathbf{j}}^{n}-\Delta t\sum_{\boldsymbol{x}_{\mathbf{j}+\frac{1}{2}\mathbf{k}}\in\partial D}\boldsymbol{f}_{\mathbf{j}+\frac{1}{2}\mathbf{k}}^{n+\frac{1}{2}}\cdot\hat{\boldsymbol{n}}_{\mathbf{j}+\frac{1}{2}\mathbf{k}}.$$

This form of discrete conservation is not a necessary condition for convergence to a weak solution of Eq. (1) [9]. Instead, a properly convergent scheme need only satisfy Eq. (11) approximately, provided the discrepancy vanishes with mesh refinement. Otherwise, $\boldsymbol{q}$ can converge to a solution of a conservation law with a fictitious source term [21]. In the next subsection, a particular departure from the discrete conservation property is explored to give a natural numerical dimension to the framework initiated in Subsection (2.2).

3.2 Multiple Overlapping Domains.

Using the Chimera technique, the following discrete form of Eq. (5) is obtained,

$$\text{(12)}\quad\begin{cases} V_{\mathbf{j}}[\boldsymbol{q}_{\mathbf{j}}^{(i),n+1}-\boldsymbol{q}_{\mathbf{j}}^{(i),n}]=-\Delta t\displaystyle\sum_{|\mathbf{k}|=1}\boldsymbol{f}_{\mathbf{j}+\frac{1}{2}\mathbf{k}}^{(i),n+\frac{1}{2}}\cdot\hat{\boldsymbol{n}}_{\mathbf{j}+\frac{1}{2}\mathbf{k}},\\ \qquad D_{\mathbf{j}}\in\Omega^{(i)},\quad t^{n+1}\in[0,T]\\ \boldsymbol{q}_{\mathbf{j}}^{(i),n+\frac{1}{2}}=\left(\tau_i\boldsymbol{q}^{(j)}\right)_{\mathbf{j}}^{n+\frac{1}{2}},\\ \qquad \partial D_{\mathbf{j}}\cap\gamma_i^j\neq\emptyset,\quad t^{n+\frac{1}{2}}\in[0,T]\\ \boldsymbol{f}_{\mathbf{j}+\frac{1}{2}\mathbf{k}}^{(i),n+\frac{1}{2}}=\boldsymbol{F}(\boldsymbol{Q}_B(\boldsymbol{x}_{\mathbf{j}+\frac{1}{2}\mathbf{k}},t^{n+\frac{1}{2}})),\\ \qquad \boldsymbol{x}_{\mathbf{j}+\frac{1}{2}\mathbf{k}}\in[\partial\Omega^{(i)}\cap\partial\Omega],\quad t^{n+\frac{1}{2}}\in[0,T]\\ \boldsymbol{q}_{\mathbf{j}}^{(i),0}=\boldsymbol{Q}_0(\boldsymbol{x}_{\mathbf{j}},0),\\ \qquad \boldsymbol{x}_{\mathbf{j}}\in\Omega^{(i)},\quad t=0\\ \qquad i=1,\ldots,I. \end{cases}$$

Here, τ_i is a data transfer operator, usually involving some form of interpolation. Since $\boldsymbol{f}^{(i),n+\frac{1}{2}}_{\mathbf{j}+\frac{1}{2}\mathbf{k}}$ may depend upon several values of $\boldsymbol{q}^{(i)}$ in a neighborhood of $\boldsymbol{x}_{\mathbf{j}+\frac{1}{2}\mathbf{k}}$, $\boldsymbol{q}^{(j)}$ values may be transferred to $\boldsymbol{q}^{(i)}$ throughout a *fringe region*, $\mathcal{F}^{(i)}$, in $\Omega^{(i)}$ near γ^j_i instead of just at γ^j_i. As a result, numerical fluxes can be evaluated near artificial boundaries in the same way as in the interior. Note that a discrete conservation property holds on each subdomain, i.e., for all $D \subset [\Omega^{(i)} - \mathcal{F}^{(i)}]$,

$$\sum_{D_{\mathbf{j}} \in D} V_{\mathbf{j}} \boldsymbol{q}^{(i),n+1}_{\mathbf{j}} = \sum_{D_{\mathbf{j}} \in D} V_{\mathbf{j}} \boldsymbol{q}^{(i),n}_{\mathbf{j}} - \Delta t \sum_{\boldsymbol{x}_{\mathbf{j}+\frac{1}{2}\mathbf{k}} \in \partial D} \boldsymbol{f}^{(i),n+\frac{1}{2}}_{\mathbf{j}+\frac{1}{2}\mathbf{k}} \cdot \hat{\boldsymbol{n}}_{\mathbf{j}+\frac{1}{2}\mathbf{k}}. \tag{13}$$

In this sense, the scheme is said to be piecewise conservative.

The system shown in Eq. (12) is solved iteratively by using the Schwarz Alternating Procedure [6]. Specifically, for a given time step, and a given subdomain, the discrete equations are solved using fixed values from other subdomains. This step is performed for all subdomains. A subiteration can be used to enhance the quality of values for the current time step. Finally, the process is repeated for a sequence of time steps until time T is reached.

A comparison of Eqs. (5) and (8) with Eq. (12) indicates that τ_i should be designed so that $\tau_i \boldsymbol{q}^{(j)}$ approximates $\mathcal{T}_i \boldsymbol{Q}^{(j)}$ on $\gamma^j_i \times [0, T]$. Also, comparing Eqs. (6) and (7) with Eq. (13) shows that $\boldsymbol{f}^{(i),n+\frac{1}{2}}_{\mathbf{j}+\frac{1}{2}\mathbf{k}}$ should approximate $\boldsymbol{F}(\mathcal{T}_i \boldsymbol{Q}^{(j)})$ on artificial boundaries. However, this follows from the consistency and continuity of the numerical flux function if $\tau_i \boldsymbol{q}^{(j)}$ converges to $\mathcal{T}_i \boldsymbol{Q}^{(j)}$. As discussed following Eq. (8), $\tau_i \boldsymbol{q}^{(j)}$ should not involve an average of $\boldsymbol{q}^{(j)}$ values from opposite sides of a shock situated at $\partial\Omega^{(i)}$. The proposed choice is for $\tau_i \boldsymbol{q}^{(j)}$ to be constructed using an essentially non-oscillatory (ENO) interpolation [22] of $\boldsymbol{q}^{(j)}$ values. Specifically, in the presence of a discontinuity at the boundary, the ENO interpolant is formed from values on only one side of the jump; otherwise, the ENO interpolant is formed in a standard way for a smooth function.

A detailed proof of convergence for the Chimera scheme will not be given here. Nevertheless, a Lax-Wendroff type convergence argument can be outlined as follows. First, let $P^{(i)}$ be some kind of projection operator onto the functions that are constant on each element $D_{\mathbf{j}} \in \Omega^{(i)}$. Then assume that artificial boundary conditions are set according to:

$$\boldsymbol{q}^{(i)}|_{\partial\Omega^{(i)}} = P^{(i)} \boldsymbol{q}^{(j)}|_{\partial\Omega^{(i)}}. \tag{14}$$

Now for some norm, $\|\cdot\|_\Omega$, which measures functions on Ω, assume that for all j,

$$\|\boldsymbol{Q}^{(i)} - P^{(j)} \boldsymbol{q}^{(i)}\|_{\Omega^{(i)} \cap \Omega^{(j)}} \longrightarrow 0 \text{ as } h \to 0 \tag{15}$$

where h is a standard measure of spatial discretization. In other words, $\boldsymbol{q}^{(i)}$ converges to $\boldsymbol{Q}^{(i)}$ not only on the $\Omega^{(i)}$ mesh but on all other overlapping meshes too. Next, let $\|\cdot\|_{\partial\Omega}$ be a norm for functions on $\partial\Omega$ for which a standard trace estimate holds [18]:

$$\|\mathcal{T}_i Q\|_{\partial\Omega^{(i)}} \leq K \|Q\|_{\Omega^{(i)}}. \tag{16}$$

It must now be shown that $\{\boldsymbol{Q}^{(i)}\}$ satisfy their respective integral equations, and that

$$\mathcal{T}_i \boldsymbol{Q}^{(i)}|_{\partial\Omega^{(i)} \cap \Omega^{(j)}} = \mathcal{T}_i \boldsymbol{Q}^{(j)}|_{\partial\Omega^{(i)} \cap \Omega^{(j)}}. \tag{17}$$

Here it is assumed that the norm, $\|\cdot\|_\Omega$, is sufficient so that Eq. (15) can be used to show, in a standard way, that the $\{\boldsymbol{Q}^{(i)}\}$ satisfy their respective integral equations. On the other hand, to establish Eq. (17), the difference between the two sides is estimated on $\gamma = \partial\Omega^{(i)} \cap \Omega^{(j)}$ as follows. First, by the triangle inequality and Eq. (14),

$$\begin{aligned} \|\mathcal{T}_i \boldsymbol{Q}^i - \mathcal{T}_i \boldsymbol{Q}^j\|_\gamma &\leq \|\mathcal{T}_i \boldsymbol{Q}^i - P^{(i)} \boldsymbol{q}^{(i)}\|_\gamma + \|P^{(i)} \boldsymbol{q}^{(j)} - \mathcal{T}_i \boldsymbol{Q}^j\|_\gamma \\ &= \|\mathcal{T}_i [\boldsymbol{Q}^i - P^{(i)} \boldsymbol{q}^{(i)}]\|_\gamma + \|\mathcal{T}_i [P^{(i)} \boldsymbol{q}^{(j)} - \boldsymbol{Q}^j]\|_\gamma. \end{aligned}$$

Here, the last equality follows since a piecewise constant function on $\omega = \Omega^{(i)} \cap \Omega^{(j)}$ is equal to its trace value on γ. Finally, according to Eq. (15), the last two terms can be estimated as follows:

$$\begin{aligned} \|\mathcal{T}_i \boldsymbol{Q}^i - \mathcal{T}_i \boldsymbol{Q}^j\|_\gamma &\leq K \|\boldsymbol{Q}^{(i)} - P^{(i)} \boldsymbol{q}^{(i)}\|_\omega + K \|P^{(i)} \boldsymbol{q}^{(j)} - \boldsymbol{Q}^{(j)}\|_\omega \\ &\longrightarrow 0 \text{ as } h \to 0. \end{aligned}$$

Thus, Eq. (17) follows. As a result, $\{\boldsymbol{Q}^{(i)}\}$ provide a multi-valued weak solution on Ω. Provided the connectivities $\{\gamma^j_i\}$ are appropriately specified, the multi-valued solution $\{\boldsymbol{Q}^{(i)}\}$ can be used to construct a global weak solution $\boldsymbol{Q}$ on Ω.

The secondary purpose of this paper can now be addressed. The fact that the Chimera scheme does not satisfy a global discrete conservation property has been labeled as the source of anomalies observed in computational experiments. Specifically, it has been claimed that the Chimera scheme fails to capture shocks properly on multiple mesh systems [11], [12], [23]. However, proper experimental technique is often lacking in such tests. Several sources of numerical error are brought together simultaneously without isolating their respective contributions to observed results.

For example, when a wave propagates from one mesh to another with different resolution, spurious waves can emerge at the interface. This observation is not linked in an essential way to data transfer errors at artificial boundaries. Indeed, the same phenomenon can be demonstrated on a single domain with a sudden change in the distribution of mesh points. In [5], Thompson et al., show that sudden variations in mesh point distributions affect the accuracy of numerical approximations. In [24], Trefethen shows that at mesh spacing discontinuities, numerical errors emerge and do not vanish with mesh refinement. Also, see the review paper by Vichnevetsky [25].

The emergence of spurious waves at artificial boundaries can also be related to the choice of numerical flux approximation. Unfortunately, this phenomenon too has been mistakenly associated with a failure of the Chimera scheme to satisfy the discrete conservation property. Specifically, in [26], Roberts reports on oscillations generated by flux-difference splitting schemes when applied to systems of nonlinear, hyperbolic equations. He identifies the source of the numerical errors to be the excitation of nonphysical intermediate states between opposite sides of a slowly moving shock. Such intermediate states can be introduced in the Chimera scheme with a poor interpolation method. These errors can be avoided with a good approximation to the trace operator, without enforcing the discrete conservation property across artificial boundaries.

In addition, when a wave crosses an artificial boundary, an explicit data transfer operation can cause the emergence of the wave on the recipient subdomain to lag behind the propagation on the donor subdomain. For steady-state problems, the effect may be unimportant. However, if the steady state contains a standing wave within an overlap region, the global

convergence of the flow field can deteriorate significantly. To avoid such temporal synchronization issues for steady state and time-accurate flow fields, the ENO interpolation should be performed in space-time.

Finally, as mentioned in the Introduction, anomalies related to insufficient dissipation near artificial boundaries have been mistakenly attributed to the non-conservative nature of a Chimera data transfer scheme. Specifically, such problems were reported in [2] where the numerical dissipation was reduced from fourth order to second order at field points too close to artificial boundaries to permit the larger stencil. It is now recognized that a poor interpolation of the conserved variables near a shock can introduce nonphysical states that excite modes along characteristics emerging from the shock. Without sufficient dissipation, the emerging waves can corrupt the flow field. Using the fringe region approach discussed above allows a consistent use of fourth order dissipation at every field point. In this way, agreement has been achieved between a flow field computed on a single domain and one computed on multiple overlapping subdomains [27]. It remains to apply the proposed ENO transfer operator to such a problem. Note that anomalies associated with switches in the difference scheme are not linked in a necessary way to domain decomposition. Such problems can be realized and treated on a single domain too.

All the above sources of error have been present simultaneously in well-known computational tests of the Chimera scheme. Clearly, to understand the nature of reported anomalies, it will be necessary to perform investigations designed to isolate the sources of error. Such investigations have been successfully initiated in Ref. [28].

4 Conclusion.

A new framework was developed here which now permits the proper analysis of Chimera schemes. Distinctions were made between the system of partial differential equations posed for a single domain and the system posed for multiple overlapping domains. As a result, a trace operator was identified as the boundary operator required for the proper transfer of values at artificial boundaries. Also, an ENO interpolation operator was proposed as a numerical approximation to the trace operator. It remains to develop a complete convergence theory built upon the established framework. Nevertheless, the fact that Chimera schemes do not generally satisfy the discrete conservation property is not seen as an obstacle to the needed convergence theory. In addition, this paper emphasizes the importance of clarifying the nature of numerical errors observed with the Chimera scheme. One class of errors is associated with a poor approximation to the trace operator. Such problems are linked in a necessary way to the domain decomposition technique. Other errors may be mistakenly attributed to some non-conservative aspect of the Chimera scheme. These phenomena are readily identified when they can be shown to be as much an issue in a single domain context as they are in the context of multiple overlapping subdomains.

References

[1] Steger, J. L., Dougherty, F. C., and Benek, J. A., *A Chimera Grid Scheme*, Advances in Grid Generation, **ASME FED** Vol. 5, June 1983.

[2] Benek, J. A., Steger, J. L., and Dougherty, F. C., *A Chimera Grid Embedding Technique with Application to the Euler Equations*, AIAA Paper No. 83-1944CP, July 1983.

[3] Benek, J. A., Bunning, P. G., and Steger, J. L., *A 3-D Chimera Grid Embedding Technique*, AIAA Paper No. 85-1523CP, July 1985.

[4] Benek, J. A., Donegan, T. L., and Suhs, N. E., *Extended Chimera Grid Embedding Scheme with Application to Viscous Flows*, AIAA Paper No. 87-1126CP, June 1987.

[5] Thompson, J. F., Warsi, Z. U. A., and Mastin, C. W., **Numerical Grid Generation Foundations and Applications**, North-Holland, New York, 1985.

[6] Schwarz, H. A., *Gesammelte Mathematische Abhandlungen*, Vol. 2, Springer, Berlin, 1890, pp. 133-134.

[7] Rai, M. M., *A Conservative Treatment of Zonal Boundaries for Euler Equation Calculations*, AIAA Paper No. 84-0164, January 1984.

[8] Berger, M. J., *On Conservation at Grid Interfaces*, ICASE Report 84-43, NASA Langley Research Center, Hampton, VA, 1984.

[9] Cheshire, G. and Henshaw, W. D., *Conservation on Composite Overlapping Grids*, IBM Research Report RC 16531 (#73446), T. J. Watson Research Center, Yorktown Heights, NY, February, 1991.

[10] Moon, Y. J. and Liou, M. S., *Conservative Treatment of Boundary Interfaces for Overlaid Grids and Multi-Level Grid Applications*, AIAA Paper No. 89-1980CP, June 1989.

[11] Wang, Z. J. and Yang, H. Q., *A Unified Conservative Zonal Interface Treatment for Arbitrarily Patched and Overlapped Grids*, AIAA Paper No. 94-0320, January 1994.

[12] Liou, M. S. and Kao, K. H., *Progress in Grid Generation: From Chimera to DRAGON Grids*, NASA Technical Memorandum 106709 (ICOMP-94-19), NASA Lewis Research Center, August 1994.

[13] Lax, P. D. and Wendroff, B., *Systems of Conservation Laws*, **Communications in Pure and Applied Mathematics**, Vol. xiii, 1960, pp. 212-237.

[14] Smoller, J., **Shock Waves and Reaction-Diffusion Equations**, Springer-Verlag, New York, 1983.

[15] Temam, R., **Navier-Stokes Equations, Theory and Numerical Analysis**, North-Holland, New York, 1984.

[16] Crandall, M. G. and Majda, A., *Monotone Difference Approximations for Scalar Conservation Laws*, **Mathematics of Computation**, Vol. 34, No. 148, January 1980, pp. 1-21.

[17] Embid, P., Goodman, J., and Majda, A., *Multiple Steady State for 1-D Transonic Flow*, **SIAM Journal of Scientific and Statistical Computing**, Vol. 5, No. 1, March 1994, pp. 21-41.

[18] Evans, L. C. and Gariepy, R. F., **Measure Theory and Fine Properties of Functions**, CRC Press, Ann Arbor, 1992.

[19] Leveque, R. J., **Numerical Methods for Conservation Laws**, Lectures in Mathematics, Birkhauser Verlag, Boston, 1990.

[20] Lax, P. D., **Hyperbolic Systems of Conservation Laws and the Mathematical Theory of Shock Waves**, SIAM, Philadelphia, 1973.

[21] Hou, T. Y. and Le Floch, P. G., *Why Nonconservative Schemes Converge to Wrong Solutions: Error Analysis*, **Mathematics of Computations**, Vol. 62, No. 206, April 1994, pp. 497-530.

[22] Harten, A., Engquist, B., Osher, S., and Chakravarthy, S. R., *Uniformly High Order Accurate Essentially Non-oscillatory Schemes, III*, **Journal of Computational Physics**, Vol. 71, 1987, pp. 231-303.

[23] Pärt-Enander, E. and Sjögreen, B., *Conservative and Non-conservative Interpolation Between Overlapping Grids for Finite Volume Solutions of Hyperbolic Problems*, **Computers and Fluids**, Vol. 23, No. 3, 1994, pp. 551-574.

[24] Trefethen, L. N., *Group Velocity in Finite Difference Schemes*, **SIAM Review**, Vol. 24, No. 2, April 1982, pp. 113-136.

[25] Vichnevetsky, R., *Wave Propagation Analysis of Difference Schemes for Hyperbolic Equations: A Review*, **International Journal for Numerical Methods in Fluids**, Vol. 7, 1987, pp. 409-452.

[26] Roberts, T. W., *The Behavior of Flux Difference Splitting Schemes Near Slowly Moving Shock Waves*, **Journal of Computational Physics**, Vol. 90, 1990, pp. 141-160.

[27] Benek, J. A., *Chimera Grid Applications*, Short Course Notes from Short Course on Advances in Grid Generation held at Mississippi State University, August 1991.

[28] Keeling, S. L., Ly, H. V., Pinter, G. A., Rogers, K. A., Rosario, R. C. D., Scroggs, J. S., Vaughan, D. E., *Modeling the Chimera Domain Decomposition Approach to Solving Conservation Laws*, Industrial Mathematics Modeling Workshop, Center for Research in Scientific Computation, North Carolina State University, August 7-16, 1995.